

Experimental study on new unbonded post-tensioned precast connection

Part 2: Experimental test with improved connection system

Yokohama National University

Member

○ Do Tien Thinh

Member

Kondo Chikako

Tasai Akira

1. Introduction

This study is the continuity of the study presented in ³⁾, named Phase 1. From the experimental results of the specimens in the Phase 1, it can be seen that the unbonded post-tensioned precast concrete connection with shear bracket has high possibility to apply for the office building. However, there were still some undesirable behaviour of the specimens with shear bracket. The aim of this study, named Phase 2, is to improve the design of the connection in the Phase 1 to obtain enhanced performance and avoid unexpected failure modes. Moreover, shear friction at the beam to column interface was also investigated again.

2. Design of Specimens

There were three specimens in the Phase 2 study, named SP1-A, SP2-A, and SP3-A. These specimens corresponded to specimens SP1, SP2, and SP3 in the Phase 1. The specimen with slab and spandrel beam was not included in this study. The brief outline and specifications of the specimens are shown in Table 1. Reinforcement detail of the specimens is shown in Fig. 1.

Shear strength of the bracket and the volume of PC bars were calculated in the same way as in Phase 1. Hence, the shear resistant area of the bracket and volume of the PC bars of the specimens in the Phase 2 were same with those of specimens in the Phase 1.

As seen from the test result of the specimens in the Phase 1, the top of the bracket was deformed after the test, caused by large concentrated stress exceeded the yield strength of the steel material. Therefore, the shear bracket should be designed for not only strength but also deformation.

The compressive stress at the top of the bracket should be checked to satisfy following condition:

$$\sigma_u = \frac{Q_u}{a} \leq \sigma_y \quad (1)$$

Where:

σ_u = ultimate compressive stress at the top of the bracket (N/mm²)

a = area of the top face of the bracket (mm²)

σ_y = yield strength of the steel (N/mm²)

In order to satisfy Eq. (1), shear bracket was modified to T-shaped with top horizontal plate. The width of this plate was 80 mm for the bracket of specimen SP2-A and 110mm for the bracket of specimen SP3-A.

For the inverted U-shaped steel box, beside the design formulars used in Phase 1, the top horizontal plate of the steel box should be designed for bending moment caused by the reaction force from the shear bracket. In order to prevent the flexural deformation, maximum tensile stress at the top face of the horizontal plate should not exceed the yield strength of the steel material:

$$\sigma \leq \sigma_y \quad (2)$$

Where:

σ = Maximum tensile stress at the upper face of the top plate (N/mm²)

Table 1 Specimens outline

Specimens		SP1-A	SP2-A	SP3-A
Beam	Section (mm ²)	300 x 500		
	F_c (N/mm ²)	69.9	60.4	68.6
	f_y (N/mm ²)	339.1	339.1	339.1
	f_{wy} (N/mm ²)	313.1	313.1	313.1
	PC bars	2- ϕ 15 Grade C	2- ϕ 26 Grade A	2- ϕ 15 Grade C
	σ_o (N/mm ²)	1.83	4.02	1.83
	P_o/P_y	0.72	0.72	0.72
PC length (mm)		1500	1500	1500
Column	Section (mm ²)	400 x 400		
	F_c (N/mm ²)	69.9	60.4	68.6
	f_y (N/mm ²)	534.4	534.4	534.4
	f_{wy} (N/mm ²)	313.1	313.1	313.1
Bracket	a_w (mm ²)	3036	-	4950
	Length (mm)	50	-	50

Where: F_c = concrete compressive strength, f_y = yield strength of beam and column longitudinal reinforcement, f_{wy} = yield strength of beam and column lateral reinforcement, σ_o = initial concrete beam stress, P_o = initial prestressed force, P_y = yield strength of the PC bar, a_w = shear resistance area of the bracket.

σ_y = Yield strength of the steel (N/mm²)

In order to satisfy Eq. (2), thicker plate (T25) and strengthen plates was used at the top of the steel box. Photos of the shear bracket and U-shaped steel box are shown in Fig. 2.

From the test result of the specimens in the Phase 1, the top part of the beam near the column face was severely damaged. Therefore, two $\phi 6$ -D150 interlock steel spirals were used at the top corner of the beam, to confine the concrete and prevent the compressive failure of the concrete at this area.

Test set up is shown in Fig.3. Detail of the set up can be found in (3).

3. Experimental Results and Discussions

3.1 Visual observation

Fig. 4 shows the crack patterns of the specimens at 4% drift angle. The bracket and beam socket after the test were shown in Fig. 5. Very few cracks occurred in all specimens at story drift of 4%. There was nearly no flexural crack occurred in the columns of all specimens. Only some shear cracks occurred in the joint area and almost closed when the loading was removed. The crushing of concrete at the top of the beam near the column face was significantly reduced compared to specimens in the Phase 1.

As seen in Fig. 5, the shear bracket and beam socket were not suffered from any damage or deformation, although they have experienced very large vertical load and high drift level. Especially in specimen SP3-A where the gravity load was 1.5 times larger than that in other specimens. Furthermore, in the case of specimens with shear bracket, it was very easy to separate the beam out of the column after the test, confirmed that this type of structural is easy to disassemble.

3.2 Hysteresis behavior

The hysteresis characteristics of the specimens are shown in Fig. 6 as the relationship between the moment and drift angle. The superimposed dashed lines on this figure illustrate the hysteresis behavior and modeled as tri-linear skeleton curve. The moment and rotation angle at the breaking points were determined as follow:

The first breaking point:

$$M_s = \frac{1}{2} \left(1 - \frac{\eta_e}{0.85} \right) \eta_e B D^2 \sigma_B \quad (3)$$

$$R_s = \frac{M_s}{3EI L} \quad (4)$$

The second breaking point:

$$M_y = \frac{1}{2} \left(1 - \frac{\eta_y}{0.85} \right) \eta_y B D^2 \sigma_B \quad (5)$$

$$R_y = \frac{\Delta \epsilon_{PC}}{0.5D} L_{PC} + \frac{M_y}{3EI L}, \Delta \epsilon_{PC} = \epsilon_{py} - \epsilon_{pe} \quad (6)$$

The end point: $M_u = M_y$.

$$R_u = \frac{\Delta \epsilon_{PC}}{0.5D} L_{PC} + \frac{M_y}{3EI L}, \Delta \epsilon_{PC} = \epsilon_{pu} - \epsilon_{pe} \quad (7)$$

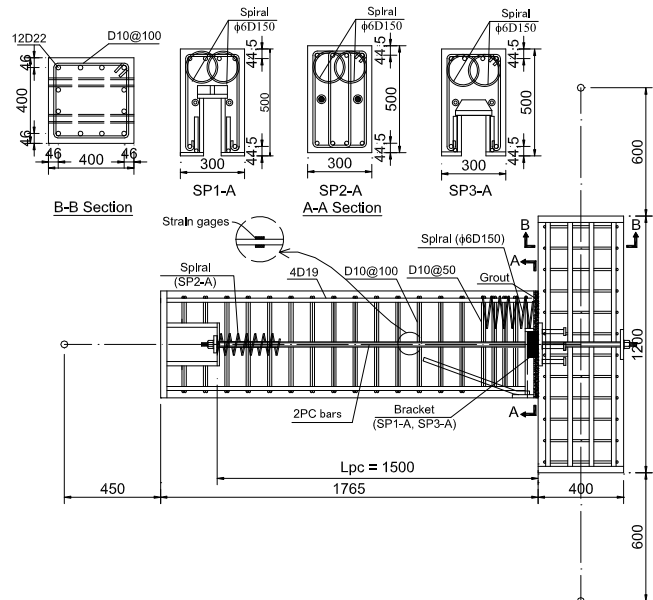


Fig. 1 Reinforcement details of the specimens



SP1-A SP3-A
Fig. 2 Photos of the shear bracket and U-shaped steel box

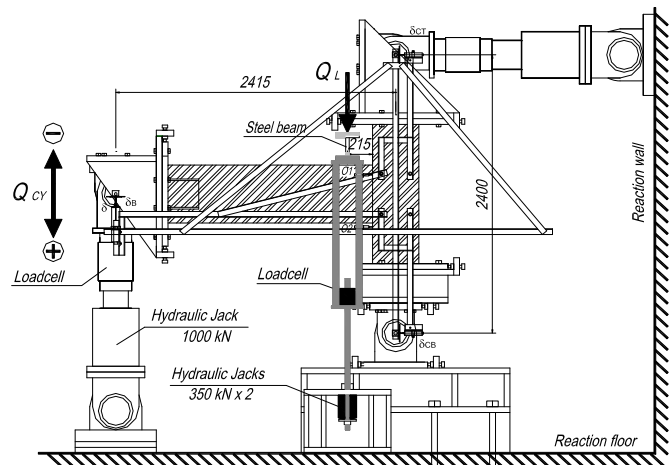


Fig. 3 Test setup

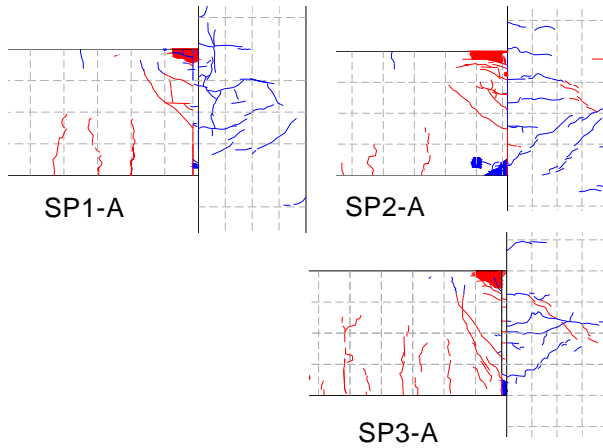


Fig. 4 Crack pattern of specimens after 4% drift



Fig. 5 Shear bracket and beam socket after tested

where:

- η_e : $= P_e / BD \sigma_B$
- P_e : initial prestress force (N)
- B, D : width and height of the beam (mm)
- σ_B : concrete compressive strength (N/mm^2)
- η_y : $= P_y / BD \sigma_B$
- P_y : PC bars yield force (N)
- L_{PC} : PC length (mm)
- E : Young modulus of the concrete (N/mm^2)
- I : second moment of the beam section (mm^4)
- L : beam length (mm)
- ϵ_{pe} : initial PC strain ($\mu\epsilon$)
- ϵ_{py} : PC strain at yielding ($\mu\epsilon$)
- ϵ_{pu} : PC strain at ultimate state ($\mu\epsilon$)

All the specimens were successfully passed the drift of 4% in negative directions and 6% in positive direction, and no fracture of PC bars was recorded. As seen in Fig. 6, while the self-centering characteristics of the specimens SP1-A and SP3-A was very good, that of specimen SP2-A was poor. The vertical slip of the beam in the specimen SP2-A was extremely large and was the cause of poor behavior of this specimen. In the specimens with shear bracket, yield moment strength well exceeded the calculated values. Average experimental yield moments were 20% and 35% larger for specimens SP1-A and SP3-A, respectively. In the specimen without shear bracket (SP2-A), while the strength in the positive direction was almost the same with the calculated one, it was 20% less than the calculated value in the negative direction. As illustrated in the

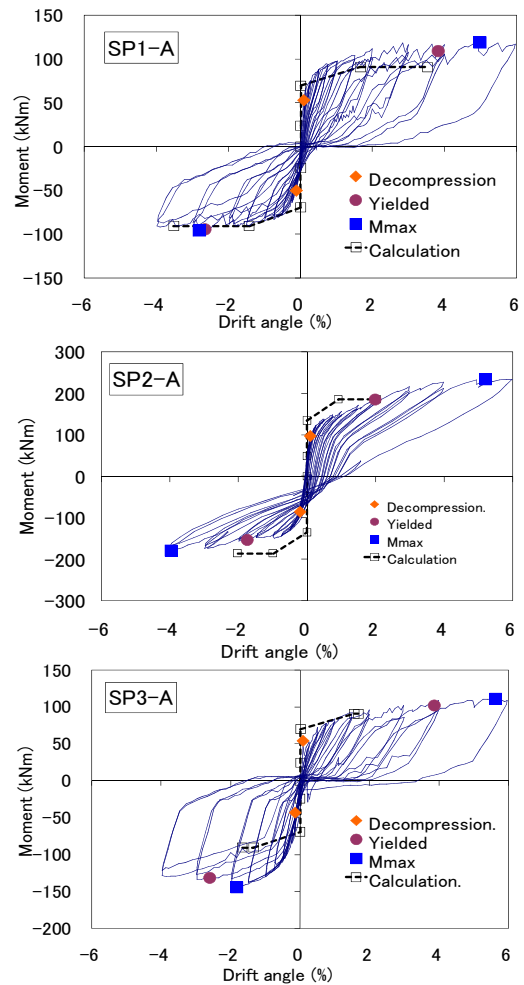


Fig. 6 Moment - rotation relationship

Fig. 7, when the beam slip occurs, the moment lever arm in the negative direction is smaller than that in the positive direction, causes the moment strength in negative direction smaller than that in the positive direction. The hysteresis curve well agreed with the computed one in the case of specimen SP1-A. Both the initial and post-yielded stiffness agrees well with the theoretical value. For the specimen

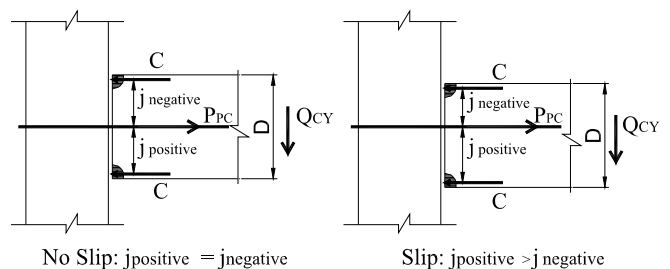


Fig. 7 Illustration of moment strength

SP2-A, the initial stiffness was less than the computed one in negative direction.

3.3 Beam slip

The beam slip – drift angle relationship of three specimens is shown in Fig. 8. It can be seen that the beam slip of specimen without shear bracket (SP2-A) was almost the same with that of specimen SP2 in the Phase 1, excessive larger than that of the specimens with shear bracket (SP1-A and SP3-A). From the test result, it concluded that the shear bracket successfully prevented the slip of the beam. Fig. 9 shows the beam slip and the Q_B/P_{PC} ratio relationship of the specimen SP2-A. The dashed line expresses the upper bound of the ratio of each loading cycle and illustrates the friction coefficient μ . It can be seen that, beam slip occurred when the value of μ was around 0.45. This value is smaller than the design value of $\mu = 0.5$. Further studies are necessary to be conducted to find out suitable value of friction coefficient.

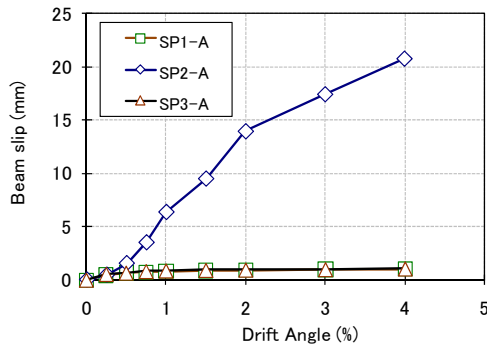
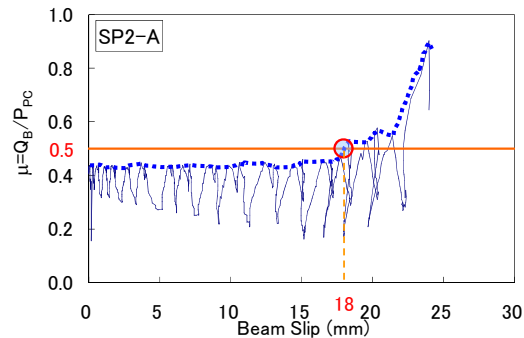


Fig. 8 Beam slips of the specimens



Q_B : Beam end shear force; P_{PC} : PC force

Fig. 9 Beam slip – friction coefficient relationship, SP2-A

4. Conclusions

Following conclusions were drawn from the experimental results of this study:

- 1) Modified shear bracket and beam socket worked well to transfer the shear force from the beam to the column, as well as satisfy the deformability of the beam at high level of drift.
- 2) The specimens with shear bracket expressed very good seismic performance, with small residual deformation, fully developed strength, nearly no beam slip and small deformation of the beam and column element, even in very long span frame. It is highly possible to apply this type of connection in real precast building structures.
- 3) The specimens without shear bracket experienced large beam slip and residual drift. The slip occurred at the friction coefficient of 0.45, smaller than design value of 0.5. Performance of the system without bracket was inferior compared to the system with shear bracket.
- 4) The slip of the beam was the cause of the difference of flexural strength between positive and negative direction.

Acknowledgement

This research was conducted as a part of the project to develop new type of high-rise R/C office building structure, coordinated by the University of Tokyo and Japan Building Contractors Society, led by Prof. Hitoshi Shiohara. The project was financially supported by Japan Ministry of Land, Infrastructure and Transport.

References

- 1) D. T. Thinh, K. Kusunoki, and A. Tasai, "Seismic Performance of Unbonded Post-Tensioned Precast Concrete Beam-Column Connection", JCI Annual Convention, Sapporo, July, 2009.
- 2) D. T. Thinh, C. Kondo, K. Kusunoki, K. Osako, T. Matsuura, N. Takamori, A. Tasai, "Development of a Large-Span Precast Concrete Structural System With Ease of Construction Using Prestressed Connections, Part 14: Discussion of Experimental Results for the Study on Large Span Exterior Connection", AIJ Annual Convention, Sendai, August, 2009.
- 3) C. Kondo, D. T. Thinh, K. Kusunoki, "アンボンド PC・PCa 圧着工法を用いた新しい柱梁接合部の開発に関する実験的研究、その 1. プロトタイプ接合部の実験結果", 18th Symposium on Development of Prestressed Concrete, Tottori, October, 2009, in Japanese.